Understanding and modeling of gas puff injection for diagnostic purposes

A. Rodriguez-Gonzalez,[1, a)] D. J. Cruz-Zabala,[1] K. McKay,[1] M. Griener,[2] U. Plank,[2] E. Viezzer,[1] V. Rohde,[2] R. Dux,[2] and the ASDEX Upgrade team[3]
[1)]*Department of Atomic, Molecular and Nuclear Physics, University of Seville, Seville, 41012, Spain*
[2)]*Max-Planck-Institut für Plasmaphysik, Garching, 85748, Germany*
[3)]*See author list of H. Zohm et al., Nucl. Fusion (2024)*

(Dated: 7 January 2025)

This contribution presents an experimental set-up capable of providing high spatial and temporal resolution measurements of neutral gas puff injection using a glow discharge to excite the neutral gas and an ultra-high-speed camera to record the emitted light. Using the proposed set-up, the shape and propagation velocity of a thermal deuterium gas puff at 1 bar has been measured. The cloud has a conical shape and a propagation velocity of $v_{prop} = 1870 \pm 270$ m/s. Furthermore, a code has been developed with the aim of studying the relation between the propagation velocity and the initial injection velocity of the gas. The simulations show that an initial injection velocity in the range of $v_{inj} \sim 1650 - 1950$ m/s can reproduce the propagation velocity of $v_{prop} = 1870 \pm 270$ m/s

I. INTRODUCTION

Diagnostics such as Gas Puff-based Charge eXchange Recombination Spectroscopy (GP-CXRS) (capable of measuring temperature, rotation velocity and density of the plasma impurities)[1–4], Gas Puff Imaging (GPI) (capable of measuring plasma edge turbulence)[5,6] and Thermal helium beam (capable of measuring electron temperature, density and edge radial electric field)[7,8] use a thermal gas puff as an active source of neutrals. These thermal neutrals are used as a simpler alternative to Diagnostic Neutral Beam Injection (DNBI) systems. Neutral particles are not deflected by the electromagnetic field and interact with the plasma, leading to light emission that can contain information about plasma parameters.

The Gas Puff based CXRS diagnostic uses a gas box inside the tokamak to inject (or puff) a thermal neutral gas that interacts with plasma impurities via charge exchange reactions. The light emitted can be analyzed with a spectrometer to calculate the temperature, rotation velocity and density of the measured impurity[1]. While impurity temperature and rotation velocity can be obtained directly from the spectrum, impurity density calculation requires information on the distribution of the injected neutrals in addition to the intensity of light. One way to obtain the neutrals penetration into the plasma is through modeling. However, this approach requires the use of an injection velocity value that is an order of magnitude lower than the theoretical thermal velocity estimation[9]. The cause of this discrepancy is still being investigated. However, since the injection velocity is currently being estimated theoretically, an experimental measurement of this velocity would be advantageous.

This contribution presents an experimental set-up capable of measuring the gas puff process with enough spatial and temporal resolution to measure the injection velocity. A glow discharge is used to excite the puffed neutral gas whose motion and shape is then measured using an ultra-high-speed camera.

This paper is structured as follows; in section II, the experimental set-up that is able to provide the necessary measurements is presented. In section III, the experimental measurements are shown and their analysis is made. In section IV, the simulation code is presented. In section V, the summary and conclusions are presented.

FIG. 1. Picture of the experimental set-up showing the blue argon plasma created by the glow discharge thorugh a vacuum window and the the high-speed camera.

II. EXPERIMENTAL SET-UP

The proposed approach to record the gas shape and its velocity is to inject the gas into a vacuum chamber where a glow discharge is present[10]. In this way, the neutral gas is excited by the cold plasma and light is emitted. This light can be analyzed with a fast camera to determine the properties of the gas

[a)]arodriguez29@us.es

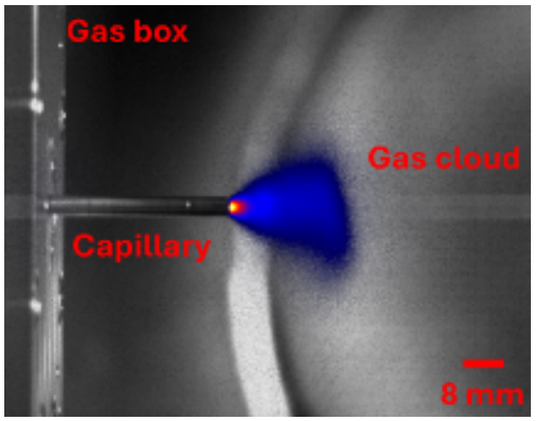

FIG. 2. Gas puff process recorded by the camera. From left to right it can be seen, the gas box where the piezo valve and the gas is contained. The capillary tube and the light emission by the gas cloud.

cloud. There are other approaches to measure the gas cloud as shown for instance in[11].

For these experiments, a vacuum chamber of around 0.5 m^3 capable of achieving pressures as low as $p_{\text{chamber}} \approx 10^{-7}$ mbar was used. A gas injection system allowed for the precise injection of argon gas into the chamber with a flow rate of 70 sccm (standard cubic centimeter per minute). Two electrodes inside the vacuum chamber initiate the glow discharge by applying a voltage of around 3 kV and then maintaining the discharge with a voltage $V_{\text{glow}} \approx 600$ V and a plasma current $I_{\text{glow}} \approx 500$ mA. With these settings, a bright blue argon cold plasma (see FIG. 1) is created inside the chamber with an arbitrary long duration, some times of several hours continuously.

The novelty of this contribution was the usage of a top-of-the-line Phantom v2512 camera[12] to record ultra-high-speed videos of the plasma. It allows recording at 25 kfps at its highest resolution of 1280 x 800 pixels and it is capable of achieving frame rates of 1 Mfps at its lowest resolution of 128 x 16 pixels. For the lens, an off-the-shelf 85mm F1.4 Sigma prime lens was used. When measuring at a resolution of 128 x 16 using such lenses, the field of view was limited to around 36.57 x 4.57 mm. To calculate the maximum velocity that could be measured, a distance of 15 mm (approximately half of the field of view) is taken as a reference, as this would leave three data points in the frame (a first data point around 0, another one around 15 mm and a last one around 30 mm). This way, the value for the maximum velocity that this set-up could measure can be calculated to be:

$$v_{max} = \frac{\Delta x}{\Delta t} \approx \frac{15mm}{1\mu s} \approx 1.5 \cdot 10^4 \text{ m/s} \qquad (1)$$

The gas puff injection is performed using a gas box with a fast piezo valve[10] (see FIG. 2). The gas box has a volume of 100 cm^3 and has a metal bellow connected to the outside of the vacuum chamber through which the gas and control cables pass. The piezo valve is actuated by applying a voltage between -20 V (fully closed) and 130 V (fully opened), which takes around 3 ms to go from the fully closed position to the fully open position. However the full gas flow rate is established approximately in 0.75 ms and remains at that level for the rest of the puff. The valve leads to a capillary tube with a length of 66 mm and a diameter of 400 µm.

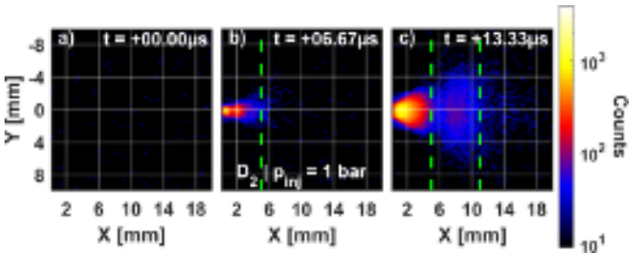

FIG. 3. First frames of the evolution of the gas cloud. The dashed green lines have been placed where the gas cloud counts over the Y = 0 mm line drop under approximately 1% of the maximum value.

III. EXPERIMENTAL MEASUREMENTS

The scenario studied is deuterium gas at 1 bar injected into an argon glow discharge. Deuterium is the gas used for the GP-CXRS diagnostic during the experimental campaign of the ASDEX Upgrade (AUG) tokamak. The gas puff pulse duration had to be limited due to safety concerns while using deuterium gas. In the case of deuterium at 1 bar, the pulse duration was 100 ms.

Using a wide resolution of 384 x 288 pixels allows to measure the shape of the whole gas cloud with a limited frame rate of 150 kfps and a field of view of around 110 x 85 mm. Some frames of the resulting video are shown in FIG. 3, where the last dark frame (a) and the two first illuminated frames (b,c) can be seen. The acquisition of the camera is synchronized with the closing of the valve and the gas takes some time to flow and emit light which means that the light emission starts somewhere in between the first dark frame and the first illuminated frame. The dashed green lines have been placed where the gas cloud counts over the Y = 0 mm line drop under approximately 1% of the maximum value. From these frames, it can be seen that the gas cloud evolves rapidly, doubling in size in one frame and almost reaching its maximum size. This fast initial evolution imposes the need of a camera that is capable of reaching much higher frame rates and motivates the measurements presented later at 1 Mfps.

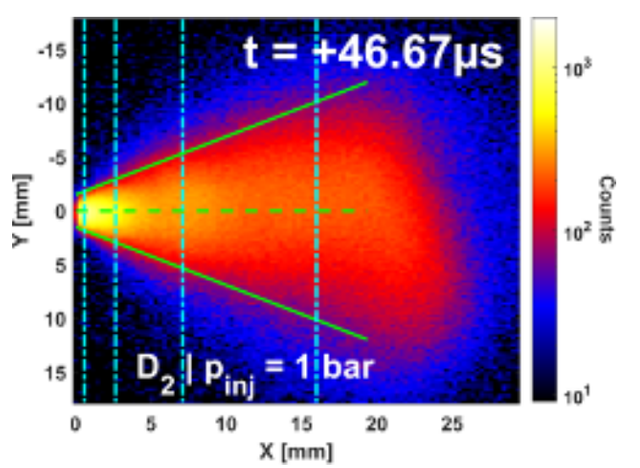

FIG. 4. The shape of the gas cloud is a cone with an angle of $\theta = 28.4 \pm 0.6$ deg. The dashed dotted cyan lines indicate the fixed X position plotted in FIG. 5 corresponding from left to right to a) through d).

In FIG. 4 a frame is shown in which the evolution of the gas shape has stopped and reached its full size. In this state, the gas cloud shape can be estimated as a cone assuming the initial shape of the cloud.

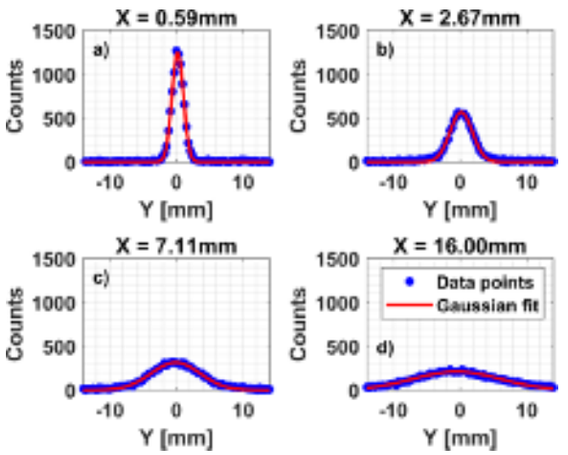

FIG. 5. Number of counts along the Y axis for four different fixed X positions. Those positions can be visualized in FIG. 4 where the subfigures a) through d) correspond in alphabetical order to the cyan lines from left to right.

If one looks at the emission profile along the Y axis (that is, for a constant X position), the normalized intensity, I_{norm} (or number of counts), is a Gaussian distribution as can be seen in FIG. 5. Thus, one can assume that the distribution in planes perpendicular to the capillary (XZ plane) is a 2D Gaussian of the following form[10]:

$$I_{\text{norm}}(x,y,z) = \frac{1}{2\pi\sigma(x)^2} \cdot \exp\left(-\frac{y^2+z^2}{2\sigma(x)^2}\right), \tag{2}$$

where σ is the standard deviation of the Gaussian. From this expression, the Full Width at Half Maximum (FWHM) can be calculated to be,

$$\text{FWHM} = 2\sigma(x)\sqrt{2\ln 2}. \tag{3}$$

The FWHM increases linearly in the x-axis starting from the injection point by the following expression,

$$\text{FWHM} = 2x \cdot \tan(\theta). \tag{4}$$

By calculating the FWHM at increasing x values, the angle θ can be obtained by linear regression of the (x, FWHM) data pairs. The first 4 data points are discarded from the interpolation, as they deviate from equation (4) as can be seen in FIG. 6. This effect is produced because particles change from flowing in a capillary tube (microscopic scale) to freely flowing in an orders of magnitude bigger vacuum vessel (macroscopic scale). The obtained angle for the cone is $\theta = 28.4 \pm 0.6$ deg. This result is higher than a previous measurement of deuterium gas at 0.6 bar which produced a cone with an angle of $\theta = 25.4 \pm 0.5$ deg[10]. The relation of this angle with the gas species and injection pressure remains to be studied further.

As seen before, when recording at 150 kfps the evolution of the gas cloud occurred rapidly during the first two frames. Thus, a higher recording speed is needed to properly evaluate the injection velocity. If the resolution is set to 128 x 16 pixels,

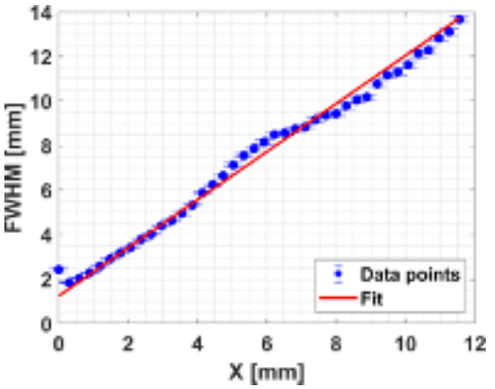

FIG. 6. Linear regression of the (x, FWHM) measurements. The first 4 points are not used in the fit due to the deviation they present from the expected equation. The deviation is expected as the particles transit from the flowing in a capillary tube to freely flowing in an orders of magnitude bigger vacuum vessel.

frame rates up to 1 Mfps are achievable and the field of view where the gas interaction process occurs is limited to 26 x 4 mm.

In FIG. 7 the first 10 frames of the gas puff injection are shown with a time resolution of 1 µs. Again, it can be observed that during the frames from 0 to 3 µs the gas cloud evolves rapidly.

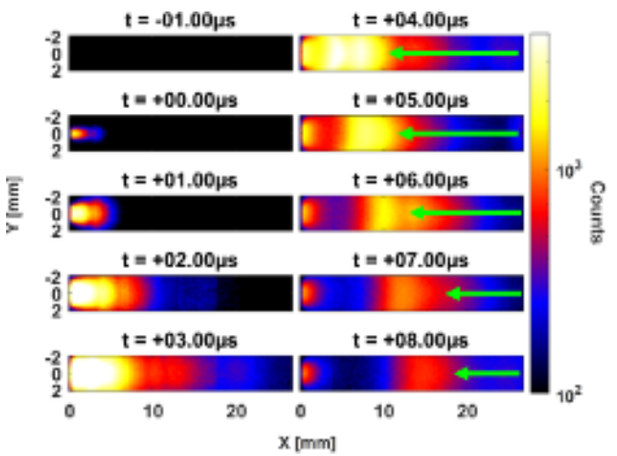

FIG. 7. First 10 frames of the gas puff recorded at 1 Mfps. In the first 3 µs the gas cloud evolves rapidly. Then, a secondary maximum or peak (indicated with a green arrow) starts to travel farther from the injection point.

However, during the experimental campaign at AUG, the gas-plasma interaction mostly occurs in the separatrix which is located 40 to 100 mm away from the capillary nozzle depending on the discharge (see FIG. 4 in reference[9]). Thus, the measurement of how fast the cloud propagates farther from the injection point is more interesting given that such velocity would be the actual velocity at the separatrix rather than the initial injection velocity.

From the frame at 5 µs on FIG. 7 onwards, a secondary maximum can be seen. This maximum, can be tracked to get a better estimation of the propagation velocity of the gas cloud. The fainter region observed in the frames from 5 to 8 µs is pro-

duced by the plasma being cooled by the neutral gas injected. The cold plasma is not capable of exciting the new gas that is being injected and thus it does not emits light. The constant injection of gas keeps this region cold enough so that the light emission does not reach the initial level anymore.

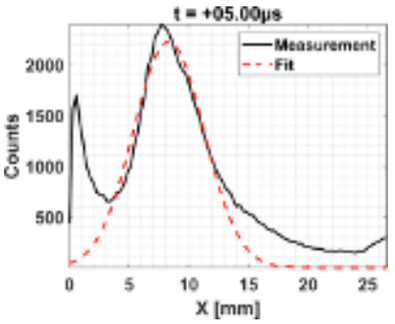

FIG. 8. Number of counts along the X axis for Y = 0 mm. As can be seen, the secondary peak has a Gaussian-like shape whose fit is indicated with a red dashed line. The lower light intensity in the region between the two peaks is produced by the plasma being cooled by the continuous injection of gas.

That peak has a Gaussian-like shape if the intensity is plotted at fixed Y = 0 mm along the X axis as can be seen in FIG. 8. A Gaussian can be fitted in each frame in order to use its centroid as an estimation of the position of the peak. The propagation velocity can be obtained by simply dividing the distance covered by the centroid from one frame to the next by the time between each frame (1 µs) and then averaging the velocities obtained between each two frames. The value obtained for the propagation velocity using this method is $v_{prop} = 1870 \pm 270$ m/s. The uncertainty is originated in the Gaussian fit and is propagated linearly. This value can be compared with theoretical estimations based on ideal gas theory. First, if one supposes that the deuterium source is thermal, then, the mean velocity is given by[13]:

$$\bar{v}_{\text{thermal}} = \sqrt{\frac{8k_BT}{\pi m}} \approx 1255 \text{ m/s}, \tag{5}$$

where k_B is the Boltzmann constant and T the temperature (300 K), and whose value is lower than the measured velocity. Another possible theoretical estimation can be given if the gas source is assumed to be an effusive source, that is, the process in which gas flow between two containers through a hole whose diameter is much smaller than the mean free path of the gas molecules[13]. For deuterium gas, the mean free path, λ, can be calculated to be[14]:

$$\lambda = \frac{k_BT}{\sqrt{2}\pi p(2r)^2} \approx 0.23 \text{ µm}, \tag{6}$$

where p is the pressure (1 bar), and r is the hard shell radius of the gas particle (~ 1 Å). The mean free path is three orders of magnitude smaller than the diameter of the capillary tube, which indicates that the gas source is not effusive. Nonetheless, if it were the case, the mean velocity is calculated by[13]:

$$\bar{v}_{\text{effusive}} = \sqrt{\frac{9\pi k_BT}{8m}} \approx 1478 \text{ m/s}, \tag{7}$$

which is compatible with the measured velocity. However, the particles can only have velocities up to a certain value given by the energy conservation for an adiabatic and isentropic supersonic expansion and has the following expression[13]:

$$\bar{v}_{\text{max}} = \sqrt{\frac{2C_pT}{m}} \approx 2084 \text{ m/s}, \tag{8}$$

where C_p is the specific heat capacity at constant pressure with a value of $C_p = 29.194 \text{ J/mol}\cdot\text{K}$[15]. Using the adiabatic sound speed, c_s, for deuterium:

$$c_s = \sqrt{\frac{\gamma\, k_BT}{m}} = 934.51 \text{ m/s}, \tag{9}$$

where γ is the specific heat ratio and is equal to $7/5$ in the case of deuterium, one can calculate the Mach number, M, using the experimental velocity measured, u:

$$M = \frac{u}{c_s} = 2.0 \pm 0.3 \tag{10}$$

which would indicate that the injection process is supersonic in the analyzed area. If friction is considered[10], then the expansion is no longer isentropic. The existence of friction could explain that the actual measured velocity is slightly lower the value calculated using equation (8).

IV. EVALUATION OF MEASUREMENTS USING A MONTE CARLO MODEL

A simulation code has been developed to study the forward propagation of a collection of particles and its relation with the initial injection velocity of the particles. Plasma interactions are not considered because it influences mainly the light emission process and not the motion of the particles. Additionally, to obtain this first approximation, the particle collisions are not considered as this makes the simulation considerably more difficult. The code initializes particles along a circle following a 2D Gaussian distribution and assigns them initial velocities in each spatial axis given by a Gaussian distribution that depends on temperature as:

$$f(v_i)d_i = \sqrt{\frac{m}{2\pi k_BT}} \exp\left\{-\frac{mv_i^2}{2k_BT}\right\} dv_i. \tag{11}$$

A constant velocity is added to the velocity given by the Gaussian distribution along the injection axis which will be called the injection velocity. Thus, the only contribution to the motion of particles is given by equation (11) and the constant velocity added to it and not by collisions or plasma interactions.

New particles are created in each time step and they are evolved in the following time steps along the existing ones. To study the propagation velocity far from the injection point, a constant number of particles are injected during the first 4 time steps and stopped thereafter. When running a simulation (using a injection velocity of $v_{inj} = 1750$ m/s), a cloud that propagates forwards is created (see FIG. 9). As stated before, the spatial characteristics of the simulated gas cloud are different from those of the experimental measurements given that collisions and plasma interactions are not considered in this simulation.

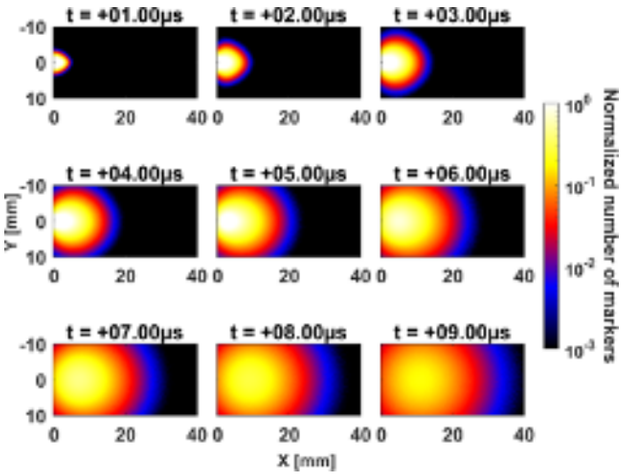

FIG. 9. Evolution of the gas cloud during 9 timesteps. Given that collisions are not simulated, the spatial spreading of the cloud is different from the experimental measurements.

FIG. 10 shows the normalized number of markers obtained by line integrating the number of particles in a line perpendicular to the viewing direction. As can be seen, the cloud only has one bright peak given that the cooling effect is not simulated. To calculate the propagation velocity, a Gaussian is fit to the simulation and its centroid is used to determine the position of the cloud. The velocity is then obtained following the same procedure than in the previous section.

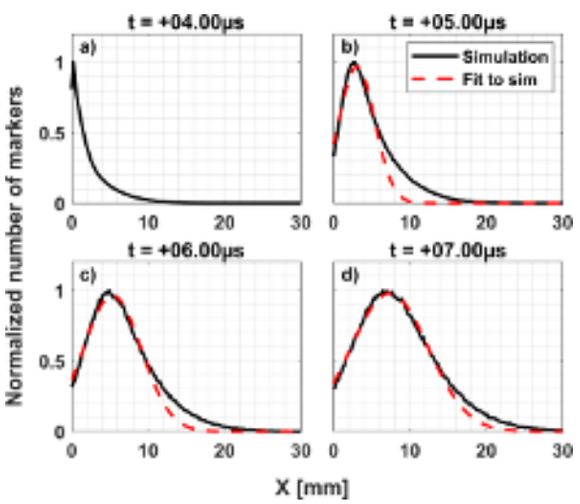

FIG. 10. Normalized number of markers along the X axis for Y = 0 mm. Subfigure a) shows the last time step where particles are being injected. By suddenly stopping the injection of particles in b), a cloud that propagates forwards is created. A Gaussian is fitted to the gas cloud, shown with a dashed red line in figures b), c) and d).

FIG. 11 shows the propagation velocity obtained after scanning the injection velocity from 1500 m/s to 2100 m/s. The red dashed lines indicates the experimentally measured propagation velocity while the green area represent its errorbar. As can be seen, the simulation predicts that to obtain the experimentally measured propagation velocity, an injection velocity of $\sim$ 1800 m/s is required. If the error bars of the experimental result are taken into account, a propagation velocity of $v_{prop} = 1870 \pm 270$ m/s can be obtained by injection velocities in the range of $1650 - 1950$ m/s.

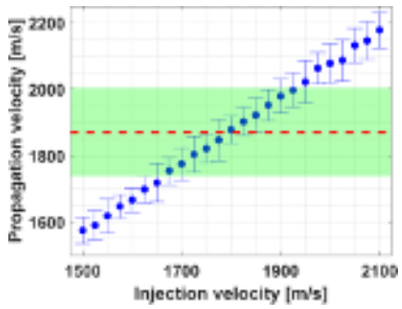

FIG. 11. Relation between the simulated injection velocity (blue points) and the measured propagation velocity. For additional context, the experimental measurement of the propagation velocity is represented with a red dashed line and its errorbar with a green shaded area.

FIG. 11 then allows for an easy determination of the injection velocity provided the measured propagation velocity in a first order approximation. Future improvements to the simulation code (for example, including particle collisions) would allow one to study this relation between velocities in more detail.

V. SUMMARY

This contribution presents an experimental set-up with high temporal and spatial resolutions that enables the measurement of the gas puff shape and injection velocity. This set-up is capable of measuring a maximum velocity of up to $1.5 \cdot 10^4$ m/s. A glow discharge is used to excite the injected neutral gas, which causes the emission of light.

When a frame rate of 150 kfps is used, the field of view of the camera allows one to measure the shape of the gas cloud, which is one of the key parameters needed for modeling the gas puff injection. When using the standard conditions of the diagnostic (deuterium gas injected at a pressure of 1 bar through the described capillary), the gas cloud takes the shape of a cone with an opening angle of $\theta = 28.4 \pm 0.6$ deg. If the frame rate is risen to 1 Mfps, then the gas puff propagation velocity can be estimated. The measurements indicate that when deuterium is injected at 1 bar, the gas propagation occurs at a velocity of $v_{prop} = 1870 \pm 270$ m/s. This result is slightly higher than the ideal gas theory calculations, but is also lower than the upper limit obtained by assuming energy conservation.

A code has been developed with the aim of finding the relation between the propagation velocity and the injection velocity of the gas cloud. In a first order approximation, particles interactions with the plasma and other particles are neglected. The addition of collisions is subject of further studies. It has been found that to reproduce a propagation velocity of $v_{prop} = 1870 \pm 270$ m/s, an injection velocity in the range of $1650 - 1950$ m/s is needed.

The set-up presented here is easily replicable and helpful to measure the interaction between neutral gases and cold plasmas. These first optical measurements of the gas puff injection velocity provides a further confirmation of the theoretical

estimations for this velocity, which is a key parameter in modeling various gas puff based diagnostics.

ACKNOWLEDGMENTS

The support from the European Research Council (ERC) under the European Union's Horizon 2020 research and innovation programme (grant agreement No. 805162) is gratefully acknowledged.

DATA AVAILABILITY

The data that support the findings of this study are available from the corresponding author upon reasonable request.

[1]R. M. Churchill, C. Theiler, B. Lipschultz, R. Dux, T. Pütterich, and E. Viezzer, Review of Scientific Instruments **84** (2013), 10.1063/1.4821084.
[2]T. Pütterich, E. Viezzer, R. Dux, and R. McDermott, Nuclear Fusion **52**, 083013 (2012).
[3]E. Viezzer, T. Pütterich, E. Fable, A. Bergmann, R. Dux, R. M. McDermott, R. M. Churchill, and M. G. Dunne, Plasma Physics and Controlled Fusion **55**, 124037 (2013).
[4]D. Cruz-Zabala *et al.*, Journal of Instrumentation **14**, C11006 (2019).
[5]S. J. Zweben, J. L. Terry, D. P. Stotler, and R. J. Maqueda, Review of Scientific Instruments **88** (2017), 10.1063/1.4981873.
[6]N. Offeddu *et al.*, Review of Scientific Instruments **93** (2022), 10.1063/5.0126398.
[7]M. Griener, E. Wolfrum, M. Cavedon, R. Dux, V. Rohde, M. Sochor, J. M. Muñoz Burgos, O. Schmitz, and U. Stroth, Review of Scientific Instruments **89** (2018), 10.1063/1.5034446.
[8]U. Plank, *The Effect of the Radial Electric Field around the Separatrix on the Access to the High Confinement Mode at ASDEX Upgrade*, Ph.D. thesis (2022).
[9]D. J. Cruz-Zabala *et al.*, Plasma Physics and Controlled Fusion **64**, 045021 (2022).
[10]M. Griener, O. Schmitz, K. Bald, D. Bösser, M. Cavedon, P. De Marné, T. Eich, G. Fuchert, A. Herrmann, A. Kappatou, T. Lunt, V. Rohde, B. Schweer, M. Sochor, U. Stroth, A. Terra, and E. Wolfrum, Review of Scientific Instruments **88** (2017), 10.1063/1.4978629.
[11]J. L. Terry, A. von Stechow, S. G. Baek, S. B. Ballinger, O. Grulke, C. von Sehren, R. Laube, C. Killer, F. Scharmer, K. J. Brunner, J. Knauer, and S. Bois, Review of Scientific Instruments **95** (2024), 10.1063/5.0219336.
[12]V. Research, "Phantom v2512 web page," `https://phantomhighspeed.my.site.com/ProductDescription?id=a0F1N00000p1K8KUAU`, [Online; accessed 18-April-2024].
[13]M. Brix, *Messung von Elektronentemperatur und -dichte mittels Heliumstrahldiagnostik im Randschichtplasma eines Tokamaks*, Ph.D. thesis (1998).
[14]R. Johnson, *Handbook of Fluid Dynamics*, Handbook Series for Mechanical Engineering (Taylor & Francis, 1998).
[15]NIST, "Nist deuterium data," `https://webbook.nist.gov/cgi/cbook.cgi?ID=C7782390&Mask=1#Thermo-Gas`, [Online; accessed 18-August-2024].